NJC

PAPER

View Article Online
View Journal | View Issue

Cite this: *New J. Chem.*, 2017, **41**, 13462

Design, synthesis, and characterisation of glyoxylamide-based short peptides as self-assembled gels†

Vina R. Aldilla, [a] Shashidhar Nizalapur, [a] Adam Martin, *[a] Chris E. Marjo, [b] Anne Rich, [b] Eugene Yee, [a] Panthipa Suwannakot, [a] David StC. Black, [a] Pall Thordarson *[a] and Naresh Kumar *[a]

Received 23rd June 2017,
Accepted 25th September 2017

DOI: 10.1039/c7nj02248d

rsc.li/njc

The synthesis and supramolecular properties of novel glyoxylamide-based short peptides formed *via* the ring-opening reaction of *N*-acetylisatins in solution phase are described. The short peptides self-assembled into gels, which were examined for their mechanical and morphological characteristics using multiple spectroscopic and microscopy techniques. The critical gel concentration and mechanical strength of the self-assembled gels were influenced by the presence of electronegative substituents (such as fluoro, in **5b**) or hydrophobic substituents (such as bromo, **5d**) respectively in the short peptides. Moreover, *in vitro* cytotoxicity assays demonstrated that these compounds were non-toxic to mammalian cells.

Introduction

Peptide-based supramolecular gelators self-assemble into nanofibres through weak intermolecular interactions including the hydrophobic effect, π–π stacking, and van der Waals forces in the presence of triggers such as pH and heat.[1] The entangled nanofibres form 3D networks that can encapsulate solvents, leading to gel formation.[2] Based on the solvent used, self-assembled gels can be categorised either as organogels or hydrogels.[3] Peptides can be designed to form supramolecular structures such as α-helices, β-sheets, and coiled-coils.[4] Additionally, self-assembled gels formed from peptides are generally non-toxic, and are typically stable under physiological conditions.[5] These qualities make them ideal for a variety of applications, including drug delivery, tissue engineering, wound healing, implant/catheter coatings, and even orifice-barrier applications.[1,6–8]

As long peptides are expensive to synthesise, attention has turned to the use of short peptides or peptide-mimics to form self-assembled gels.[4,9] Short peptides containing aromatic residues such as phenylalanine, tyrosine and tryptophan are frequently used to generate self-assembled gels due to their ability to take part in extensive π–π stacking interactions.[7,10–12] To further enhance intermolecular interactions between short peptides, additional non-proteinaceous aromatic groups are frequently incorporated.[13,14] For example, fluorenylmethyloxycarbonyl (Fmoc), which is often used as a protecting group in solid phase peptide synthesis (SPPS), is commonly incorporated at the N-terminus of diphenylalanine (FF) to enhance π–π stacking, thus driving the self-assembly process.[15–17] Besides Fmoc, other aromatic groups, such as indole, benzimidazole, and pentafluorobenzyl have been incorporated into peptide mimics.[18,19] Importantly, the choice of the aromatic "cap" can influence the mechanical and morphological characteristics of the resultant gel.[18–20]

In this work, the synthesis of novel short peptides (Fig. 1) that contain a glyoxylamide-based aromatic cap appended to the N-terminus of diphenylalanine (FF) is described. The glyoxylamide functionality was introduced *via* the ring-opening reaction of *N*-acetylisatin, creating a strong and stable linkage that also possesses the capacity to form intermolecular interactions to drive the self-assembly process.[21] Besides bearing an aromatic group, the glyoxylamide linkage also contains two carbonyl groups pointing in two different spatial directions, which introduces an additional source of H-bonding. Importantly, while most peptides designed for self-assembled gel formation are synthesised

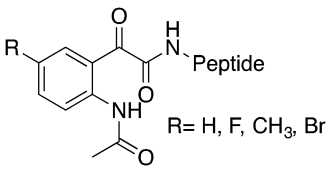

Fig. 1 Molecular design of the novel glyoxylamide-based short peptides.

[a] *School of Chemistry, UNSW Australia, Sydney, NSW 2052, Australia. E-mail: n.kumar@unsw.edu.au, adam.martin2@unsw.edu.au*
[b] *Mark Wainwright Analytical Centre, UNSW Australia, Sydney NSW 2052, Australia*

† Electronic supplementary information (ESI) available. See DOI: 10.1039/c7nj02248d

using SPPS[10,18,21–25] these glyoxylamide-based short peptides could be synthesised in solution phase, and this has the advantages of scalability and access to chemical diversity. The novel glyoxylamide-based short peptides were synthesised using either linear or parallel methods, and the yields and efficiencies of the two methods were compared. Moreover, the effects of the hydrophobicity and electronegativity of substituents at the 5-position of the acetylisatin ring C-terminus on gel formation were examined.

The self-assembly process was initiated using heat and pH as triggers. Characterisation of the self-assembled gels was performed using multiple spectroscopic and microscopy techniques to assess H-bonding interactions, secondary structure, and network morphology. The mechanical strength of the self-assembled gels was measured by conducting rheological frequency and strain sweep tests. Additionally, the cytotoxicity of glyoxylamide-based short peptides was evaluated against MRC-5 non-malignant human fibroblast cells.

Results and discussion

Synthesis of glyoxylamide-based short peptides

In the first approach, the short peptides were synthesised using the linear method as shown in Scheme 1. Isatin **1** was refluxed in acetic anhydride using a previously published protocol to generate the starting material acetylisatin **2a**.[26] Subsequently, acetylisatin **2a** was ring-opened with L-phenylalanine methyl ester hydrochloride using saturated $NaHCO_3$ solution in DCM to furnish compound **3** in 58% yield. Ester **3** was converted to acid **4** in 88% yield by hydrolysis using NaOH as a base. Compound **4** was reacted with another unit of L-phenylalanine methyl ester using HOBt and EDC·HCl in DCM at room temperature for 16 h to generate the dipeptide **5a** in 40% yield. Finally, compound **5a** underwent basic hydrolysis using NaOH in MeOH at room temperature for 16 h to generate the target compound **6a** in 86% yield.

In a parallel approach, N-Boc-protected L-phenylalanine **7** and L-phenylalanine methyl ester were first coupled together using EDC to generate the Boc-protected FF **8** in 92% yield as shown in Scheme 2. The Boc group was then easily removed using 4 M HCl in dioxane to afford compound **9** in 96% yield. The advantage of using the parallel approach is that the stable FF methyl ester hydrochloride salt **9** can be synthesised on a large scale and used for subsequent ring-opening reactions to form various acetylisatins. Thus, acetylisatins **2a–d** were ring-opened with compound **9** to generate the glyoxylamide-based dipeptides **5a–d** in moderate to high yields after column chromatographic purification. The esters **5a–d** were then subjected to basic hydrolysis to generate the target glyoxylamide-based short peptides **6a–d** in 60–82% yields and in high purity without the need for chromatographic purification. In the ^{1}H NMR spectra of the glyoxylamide-based short peptides, the glyoxylamide proton has a characteristic shift located at approximately δ 8.9 ppm.

Ring-opening reactions with the linear method were conducted using biphasic solutions as reported by Cheah *et al.*[27] However, by using acetonitrile and trimethylamine, which provide monophasic solutions, the yield of compound **5a** formed by the ring-opening reaction increased from 58% to 86%, despite the less nucleophilic nature of FF methyl ester (compared to phenylalanine methyl ester salt). Additionally, chromatographic purification was required to obtain the glyoxylamide–phenylalanine methyl ester **3** with the linear method, which was less efficient than the parallel method. This results in 1.6–2.0 times higher overall yields generated by the parallel method as compared to the linear method.

Self-assembled gel formation

Self-assembly is a process similar to crystallisation, in which a collection of molecules spontaneously forms a well-defined structure. As the gel forms, the molecules form 3D fibrous networks that can entrap the solvent. The ability of the glyoxylamide-based short peptides to immobilise solvents was

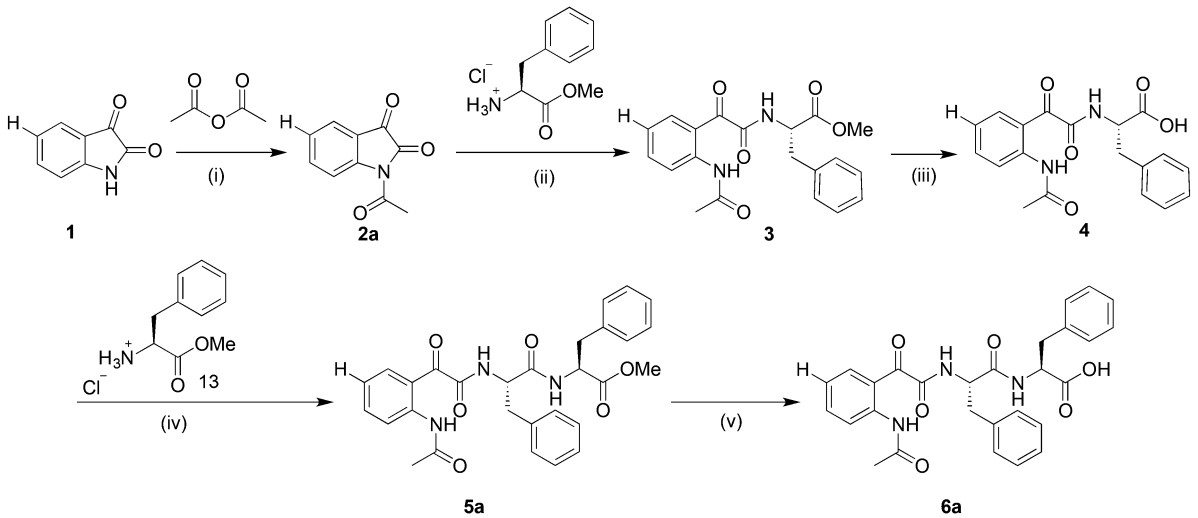

Scheme 1 Synthesis of a glyoxylamide-based short peptide *via* a linear approach. *Reagents and conditions*: (i) acetic anhydride, reflux 150 °C, 4 h (ii) sat. $NaHCO_3$ in DCM, r.t., 16 h (iii) NaOH in MeOH, r.t., 16 h (iv) EDC·HCl, HOBt, Et_3N, r.t., 16 h (v) NaOH in MeOH, r.t., 16 h.

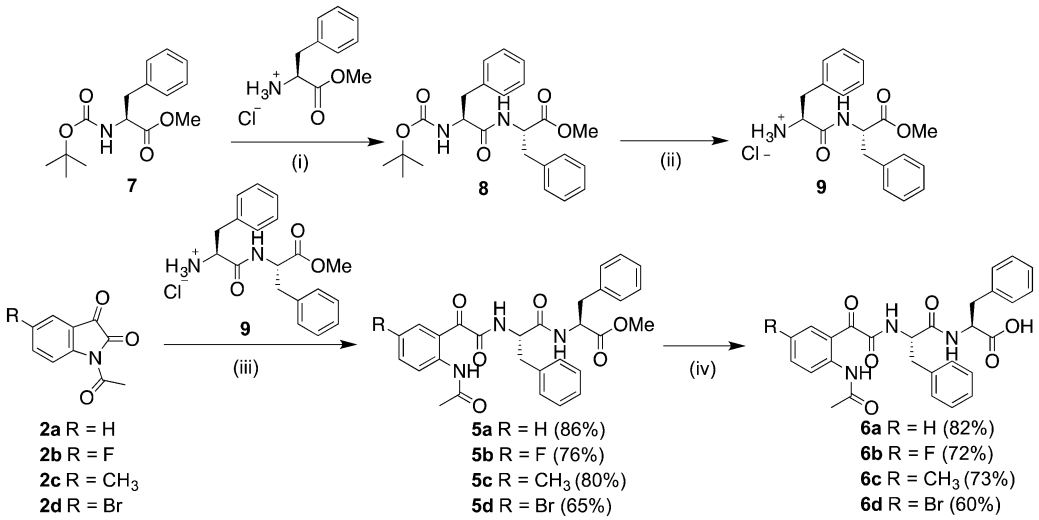

Scheme 2 Synthesis of glyoxylamide-based short peptides *via* a parallel approach. *Reagent and conditions*: (i) EDC·HCl, HOBt, Et_3N, r.t., 16 h (ii) 4 M HCl in dioxane, dry DCM, r.t., 16 h (iii) Et_3N, dry acetonitrile, r.t., 20 min to 1 h (iv) NaOH in MeOH, r.t., 16 h.

tested using several different trigger methods, such as heat, pH-switching, and solvent-switching. After applying a heat trigger, the glyoxylamide esters (**5a–d**) gelated in 2-propanol and toluene at a relatively low concentration (0.02–0.5% w/v). These organogels are thermoreversible, with gel-to-sol transition temperatures (T_g) ranging from 40–60 °C (Table 1).

In the literature, the presence of fluoro substituents on the phenylalanine moiety of a peptide gelator unexpectedly lowered their critical gel concentration (CGC).[28] Consistent with this, the fluoro-substituted compound **5b** was a super gelator, which can immobilise toluene at very low concentrations ($\leq$0.02% w/v). However, compounds **5a–d** could not be tested in water as they were insoluble, presumably due to the presence of the hydrophobic ester group at the C-terminus of the compounds. Compounds **6a–d** were expected to form hydrogels due to the presence of the carboxyl group at their C-terminus. This carboxyl group could be converted into a salt using NaOH to further increase the solubility of these compounds in water. Gelation could then be induced by lowering the pH to convert the salt back into its less soluble carboxylic acid form. However, only compound **6a** formed hydrogels at a 0.2% w/v concentration by the pH switch method using glucono-δ-lactone (GdL). The hydrolysis of GdL in water to form gluconic acid is slower than its dissolution rate.[29] Consequently, GdL yields uniform gels, compared to mineral acids.

Table 1 CGC and T_g of the glyoxylamide-based short peptide self-assembled gels

Compound	Solvent	CGC (% w/v)	Observation	T_g (°C)
5a	IPA*	0.20	Clear gel	40
	Tol**	0.05		60
5b	IPA	0.10	Clear gel	42
	Tol	0.02		57
5c	IPA	0.25	Clear gel	45
	Tol	0.07		52
5d	IPA	0.40	Opaque gel	40
	Tol	0.1		50
6a	Water	0.1	Opaque gel	N/A
6b	Water	N/A	Precipitate	N/A
6c	Water	N/A	Precipitate	N/A
6d	Water	N/A	Precipitate	N/A

The other carboxylic acid compounds **6b–d** failed to form hydrogels using a pH switching method, heating–cooling in phosphate buffered saline, or solvent switching using DMSO. This result might be attributed to their different hydrophobicities, compared to **6a**. The hydrophobicity of these molecules was predicted using a partition coefficient between the aqueous and hydrophobic phases (log*P* value). The fluoro- (**6b**), methyl- (**6c**), and bromo- (**6d**) substituted compounds have log*P* values of 2.23, 2.56, and 2.90 respectively, indicating that these compounds are significantly more hydrophobic compared to the parent compound **6a** (log*P* = 2.07). The higher log*P* values of compounds **6b–d** might interrupt the balance of hydrophobicity and hydrophilicity of the molecules, leading to precipitation instead of gel formation.[30,31]

Structural characterisation of self-assembled gels

^{1}H NMR analysis. The self-assembly process is driven primarily by the hydrophobic effect in synergy with intermolecular H-bonding interactions.[32] To understand the role of intermolecular H-bonding in driving the self-assembly, the transformation of the ^{1}H NMR for **5a** at different temperatures was investigated. The notable downfield shift ($\Delta\delta$ = 0.11–0.27 ppm) for the NH protons from **5a** was observed upon transition from the gel phase to the solution phase (Fig. 2.). The ^{1}H NMR signal of the NH capping group; NH Phe (1); and NH phe (2) were shifted downfield with $\Delta\delta$ = 0.11 ppm, $\Delta\delta$ = 0.27 ppm, and $\Delta\delta$ = 0.21 ppm respectively. The downfield chemical shift of the amide protons indicates that these NH protons contribute to intermolecular H-bonding.[33,34] In addition, the disappearance of spectral peaks at 30 °C confirmed the complete transformation from the solution phase into the gel phase.[34]

ATR-FTIR analysis. To further support the ^{1}H NMR analysis during the gel formation, an ATR-FTIR study was conducted.

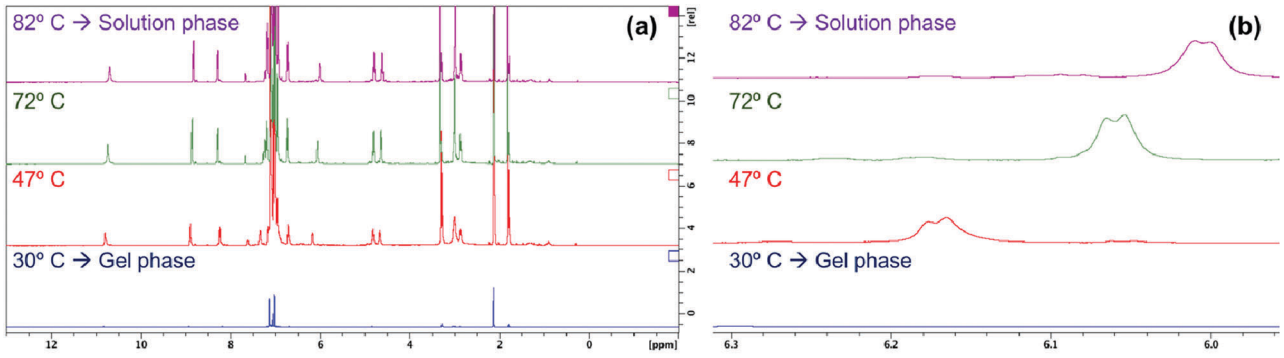

Fig. 2 ^{1}H NMR of **5a** in toluene-d_8 at temperatures ranging from 30 °C to 82 °C. (a) The overall spectra and (b) the most notable downfield shifting on NH Phe (1).

The ATR-FTIR spectrum of **5a** was compared between their xerogel (or dried gel phase) and hydrated gel phases (Fig. 3a).

The spectrum of **5a** in the gel phase was processed by subtracting the toluene spectrum to reveal the absorption peaks for **5a**. There are strong similarities between the gel phase and the xerogel phase of **5a**, with notable similarities in amide I and amide II bands. These observations confirm that the conformation of the peptide chain in **5a** is the same in both phases. The ATR-IR spectrum also confirms the presence of H-bonding (Fig S1a, ESI†), as was observed in the ^{1}H NMR. Small differences in intensities in the peaks at 1495 and 1178 cm^{-1} and additional peaks in the gel phase between 1150–950 cm^{-1} were observed that may be due to non-peptide conformational changes, such as the phenyl groups.

In addition, the gelation of **5a** in 2-propanol was also monitored at the gel-ATR crystal interface. Hence, only traces of **5a** were observed in the first 3 minutes, with the majority of peaks matching that of pure 2-propanol (Fig. 3b). However, after 20 minutes the spectrum of **5a** appeared, notably the characteristic amide at around 1600–1650 cm^{-1} and ester C=O peaks at around 1700–1750 cm^{-1}. The spectrum stabilised after 22 minutes and displayed peaks from both **5a** and 2-propanol. The strong contribution from **5a** to the final spectrum of the gel was unexpected based on the low concentration of **5a** used. It is unlikely that this increase in relative intensity was due to evaporation of 2-propanol as the measured surface of the gel was sealed against the ATR crystal. A more likely explanation is that a stable gel requires a higher concentration of gelator at the surface relative to the bulk. Fig. S1b (ESI†) shows an expansion of the carbonyl peak region after the first three minutes of measurement of **5a** gel formation in 2-propanol. There are five different carbonyl environments in compound **5a**: a benzylic ketone, a methyl ester, and three amides, hence there should be three to five peaks in this region for each type of carbonyl group.

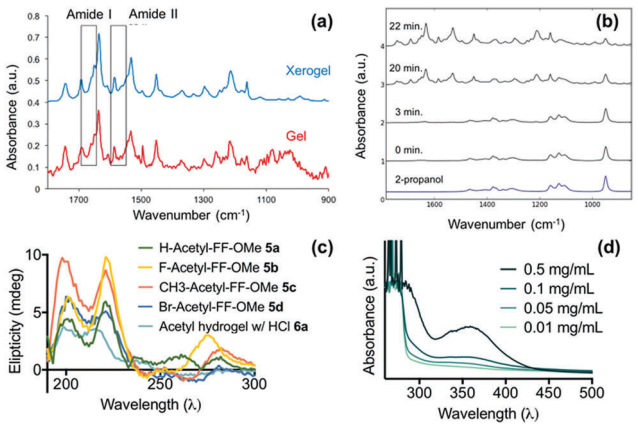

Fig. 3 (a) Stackplot of ATR-FTIR spectra of **5a** in their xerogel and gel-form, with toluene solvent subtracted. (b) *In situ* ATR-FTIR spectra of compound **5a** in 2-propanol at different time points. (c) CD spectra of glyoxylamide-based short peptide self-assembled gels showed the characteristic peak of β-sheets and random/disordered coil. (d) UV/Vis spectra of **5a** in toluene of different concentrations.

In fact, significantly more than five peaks are observed, and the relative ratio and position of each peak changes over time. One interpretation of this behaviour is that the conformer(s) of compound **5a** exhibit different peaks in solution and in the developing gel phase, and the infrared spectrum changes with the increasing proportion of compound **5a** locked in the gel phase conformation. Unlike the slow gelation of **5a** in 2-propanol, the gelation of **5a** in toluene is rapid. Hence, the *in situ* ATR-FTIR monitoring for the gelation of **5a** in toluene could not be carried out.

UV/Vis and circular dichroism (CD) analysis. Besides intermolecular H-bonding interaction, the π–π stacking of the aromatic units also has a significant influence in driving the self-assembly.[35] Therefore, the role of π–π stacking interactions from the aromatic groups of **5a** was investigated using CD spectroscopy and UV/Vis. From the previous study, the self-assembly in short peptides driven by π–π stacking interactions would typically give rise to a positive maxima around 200–218 nm in the CD spectra.[36] The positive maxima was observed (Fig. 3c) at 200 nm (π → π* transition) and 224 nm (n → π* transition), suggesting the existence of π–π stacking interactions from the aromatic units.[37,38] The CD measurements of the toluene gels were not possible due to the strong interference due to solvent absorption.

The UV/Vis spectra of a dilute sample of **5a** also showed a subtle red shift both in toluene (Fig. 3d) and 2-propanol (Fig S2a, ESI†) as the concentration increased from 0.01 mg mL^{-1} to 0.5 mg mL^{-1}. Furthermore, the shoulder peak ranging from

316 nm to 412 nm was also elevated, supporting the fact that π–π stacking interactions play a significant role in driving the self-assembly.[38,39]

Powder X-ray diffraction (pXRD)

Powder diffraction is usually performed to provide information about the molecular arrangement and microstructure of gelators. A diffraction pattern could help differentiate between crystalline and amorphous materials. No peaks in the PXRD pattern were observed for the native gel or xerogels of **5a** (Fig. S2b and c, ESI†). This suggests that no long-range order is present in the gel state for **5a**.

Secondary structure of self-assembled gels

The secondary structures of the glyoxylamide-based short peptide self-assembled **5a–d** gels were also determined using CD spectroscopy. A positive characteristic peak observed at 224 nm is typically indicative of the presence of a β-sheet secondary structure. On the other hand, the positive peaks at 200 nm suggested the presence of a random/disordered coil secondary structure (Fig. 3c). These CD peaks maxima are at a higher wavelength than the typical β-sheet and random coil secondary structures found in natural peptides (197 and 220 nm, respectively).[40] However, it should be noted that these interpretations are based on much longer peptides.[41] In addition, two FTIR peaks in the amide I region (1636 and 1650 cm^{-1}) also suggest the existence of the β-sheet and disordered coil conformation in the peptide backbone.[42]

Mechanical strength of self-assembled gels

The mechanical strength of the self-assembled gels formed from the glyoxylamide-based short peptides was evaluated using a rheometer. In the frequency sweep test, the storage modulus (G') was found to be significantly higher than the loss modulus (G'') and frequency independent, which is characteristic for a self-assembled gel. The storage modulus (G') value is commonly used as a measure of gel stiffness. As shown in Fig. 4, compounds **5a–c** exhibited similar G' values of approximately 5×10^4 Pa in 2-propanol and 3×10^4 Pa in toluene. However, the bromo compound **5d** was less stiff compared to the other organogels in either 2-propanol ($G' = \sim 2 \times 10^4$ Pa) or toluene ($G' = \sim 3 \times 10^3$). The presence of the hydrophobic bromo substituent in **5d** may interrupt the π–π stacking interaction between the aromatic groups at the N-terminus of the dipeptide[43] or possibly engage in alternative interactions not possible in **5a–c**. In addition, despite its exceptionally low CGC, the fluoro substituent **5b** does not significantly improve the mechanical strength in either organogel.

The hydrogel of compound **6a** was classed as a soft gel as indicated by its low G' value of $\sim 10^3$ Pa (Fig. 4e). In addition, its gel properties were lost at higher frequency values (>1%), where it exhibited a more liquid-like behaviour rather than gel. This behaviour was observed across multiple rheological tests.

The strain sweep test measures the material response to increasing deformation (strain) monitored at constant frequency. The linear viscoelastic region (LVER) denotes the region where the storage modulus of the gel is independent of applied strain, and is

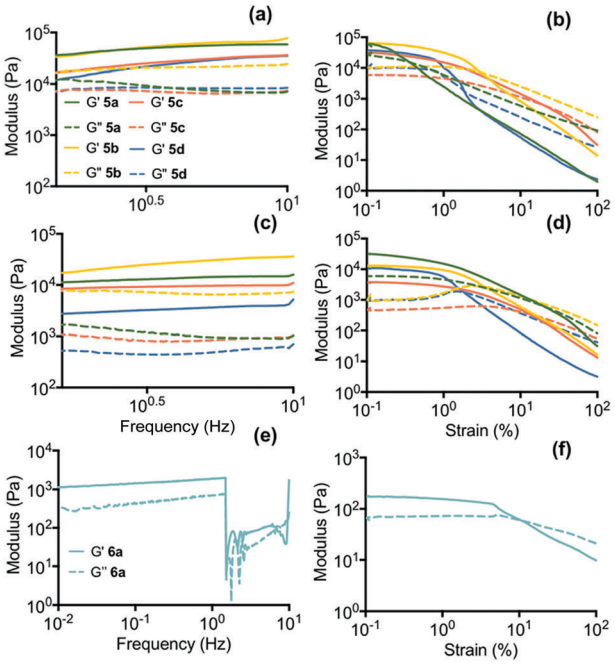

Fig. 4 Frequency sweep test (FST) and strain sweep test (SST) of glyoxylamide-based short peptide self-assembled gels. (a) FST of compound **5a–d** gels in 2-propanol (organogel). (b) SST of compound **5a–d** gels in 2-propanol (organogel). (c) FST of compound **5a–d** gels in toluene (organogel). (d) SST of compound **5a–d** gels in toluene (organogel). (e) FST of compound **6a** gel in water. (f) SST of compound **6a** gel in water.

indicative of the stability of the gel, with an extended LVER corresponding to a more stable gel. In general, compounds **5a–d** formed toluene gels with longer LVERs than the corresponding 2-propanol gels (Fig. 4). Compound **5b**, containing the small and electronegative fluorine atom, showed increased viscoelastic properties of gels which suggests that there is an electronic contribution from the fluorine atom to the π–π interactions.[44]

Network morphology of the self-assembled gels

The xerogels, or dried gels, were imaged using atomic force microscopy (AFM) to visualise the morphology of the organogel and hydrogel networks (Fig. 5). The toluene gels generally exhibited less compact networks compared to the 2-propanol gels, and this could account for their more malleable behaviour (longer LVER) compared to the 2-propanol gels in the SST. The AFM micrographs of the toluene gels at very low concentrations showed the formation of fibres with thicknesses between 18 nm to 30 nm. However, the nature of the substituent at the 5-position of the short peptide appears not to significantly affect the morphology (curvedness, bundling behaviour) of the gels. The hydrogel of compound **6a** generally formed shorter fibres compared to the 2-propanol and toluene gel generated from compound **5a–d**. The shorter fibres observed in hydrogel **6a** are consistent with their softer behaviour as shown by the rheology results.

Cytotoxicity of 6a

As prospective drug delivery agents, one requirement of these self-assembled hydrogels is possessing non/low toxicity towards

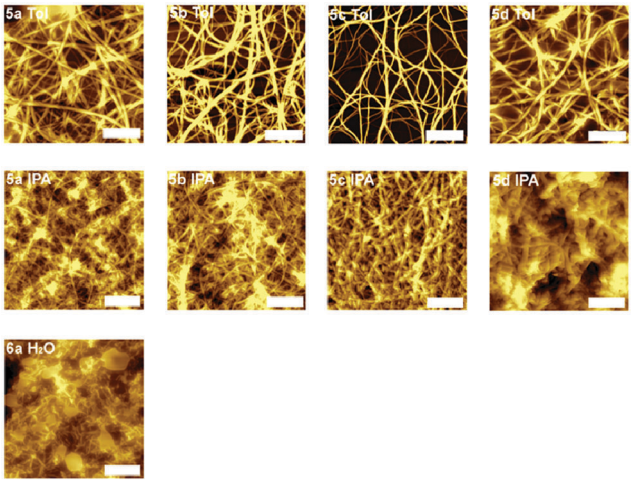

Fig. 5 AFM images of glyoxylamide-based short peptide self-assembled gels. The AFM images of the compounds were taken at concentrations four times below their CGC. (i) Compound **5a–d** gel in toluene, (ii) compound **5a–d** gels in 2-propanol, and (iii) compound **6a** in water.

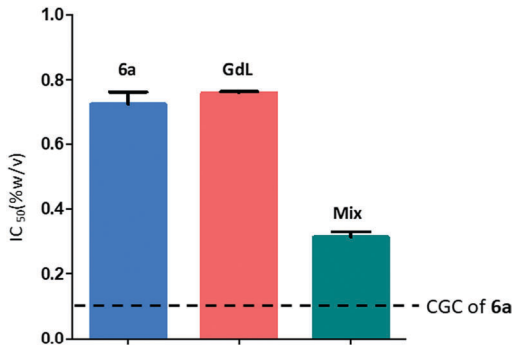

Fig. 6 Cytotoxicity of compound **6a**, GdL, and a mixture of **6a** and GdL against MRC-5 non-malignant human lung fibro blast cells.

human cells. Dipeptides such as FF and small molecules based on glyoxylamides are generally known to be non-toxic.[45–47] The cytotoxicity of the glyoxylamide based short peptide compound **6a**, which forms hydrogels, was assessed *in vitro* against normal human lung fibroblast cells MRC-5 (Fig. 6). The result showed that compound **6a** (IC_{50}: 0.73 ± 0.04% w/v) and GdL (IC_{50}: 0.76 ± 0.01% w/v) alone were non-toxic towards MRC-5 cells at very high concentrations. Although the combination of **6a** and GdL (IC_{50}: 0.31 ± 0.02% w/v) led to a decrease in the IC_{50} value, the concentration was still significantly above its CGC of 0.1% w/v. Therefore, compound **6a** is a promising candidate for future applications in topical drug delivery.

Conclusions

We have successfully synthesised novel glyoxylamide-based short peptides *via* the ring-opening reactions of *N*-acetylisatins, an approach that provides access to a wide range of derivatives in a scalable manner to better understand and optimise gelator properties. The short peptides reported herein formed self-assembled gels in toluene, 2-propanol and water. We have also examined the effect of substitution at the 5-position of short peptides on the CGC, mechanical strength, and morphology of the gels. Compound **5b** bearing a fluoro substituent showed a dramatically reduced CGC value and a longer linear viscoelastic region (LVER). In contrast, compound **5d**, with a bromo substituent, formed the softest gel among the organo-gels, suggesting that the gel properties for this family of compounds are influenced by the balance between the electronegativity and hydrophobicity of the short peptides. Despite its weak mechanical strength, the hydrogel of compound **6a** was non-toxic towards human fibroblast MRC-5 cells, suggesting potential drug delivery applications. In summary, this work has introduced a new class of short peptides with self-assembly properties which can be synthesised in large quantities, and has also shown that their gel properties can be modulated by the nature of the substituents, potentially allowing them to be useful in a variety of applications such as drug delivery.

Experimental

All chemicals and solvents used were purchased from Chemimpex and Sigma Aldrich and were used directly without any further purification.

Synthesis

Synthesis of *N*-acetylisatin derivatives 2a–d[21,27]. *N*-Acetyl derivatives **2a–d** were obtained by reacting isatin derivatives **1a–d** with acetic anhydride under reflux for 4 h. The reaction mixture was stirred at room temperature for 24 h. The yellow precipitate formed was filtered and dried to give the pure compounds **2a–d** in 78–85% yield.

1-Acetylindoline-2,3-dione **2a**: ^{1}H (400 MHz; $CDCl_3$) 8.42 (dt, J = 8.3, 0.7 Hz, 1H, *ArH*), 7.69–7.80 (m, 2H, *ArH*), 7.34 (dt, J = 7.5, 0.8 Hz, 1H, *ArH*), 2.74 (s, 3H, N $COCH_3$).

1-Acetyl-5-fluoroindoline-2,3-dione **2b**: ^{1}H NMR (400 MHz, $CDCl_3$): 8.34 (dd, J = 8.6, 0.8 Hz, 1H, *ArH*), 7.89 (d, J = 2.4 Hz, 1H, *ArH*), 7.82 (dd, 1H, J = 7.8, 2.4 Hz, *ArH*), 2.74 (s, 3H, $COCH_3$).

1-Acetyl-5-methylindoline-2,3-dione **2c**: ^{1}H NMR (400 MHz, $CDCl_3$): 8.29 (d, J = 8.4 Hz, 1H, *ArH*), 7.58 (s, 1H, *ArH*), 7.52 (dd, J = 8.4, 1.8 Hz, 1H, *ArH*), 2.42 (s, 1H, $ArCH_3$), 2.72 (s, 1H, $COCH_3$).

1-Acetyl-5-bromoindoline-2,3-dione **2d**: ^{1}H NMR (400 MHz, $CDCl_3$): 8.34 (dd, J = 8.6, 0.8 Hz, 1H, *ArH*), 7.89 (d, J = 2.4 Hz, 1H, *ArH*), 7.82 (dd, 1H, J = 7.8, 2.4 Hz, *ArH*), 2.74 (s, 3H, $COCH_3$).

Synthesis of phenylalanine phenylalanyl methyl ester salt 9. The commercially available N-Boc protected L-phenylalanine (1 eq.) was coupled with phenylalanine methyl ester hydrochloride salt (1 eq.) using hydroxybenzotriazole (HOBT) (1.2 eq.) and *N*′-ethylcarbodiimide (EDC) in DMF. The product **8** was precipitated by the addition of ice-water and the Boc-protecting group was removed using 4 M HCl (2 eq.) in dioxane to provide **9** in quantitative yield.

Methyl L-phenylalanyl-L-phenylalaninate hydrochloride salt **9**:[48] ^{1}H NMR (400 MHz, DMSO-d_6): 9.13 (1H, d, J = 7.50 Hz, *NH*), 8.16 (1H, s, *NH*), 7.24–7.32 (10H, m, *ArH*), 4.55 (1H, td, J = 10.0,

4.0 Hz, *CH*), 4.05 (1H, td, *J* = 8.4, 5.4 Hz, *CH*), 3.60 (3H, s, $COOCH_3$), 3.03–3.15 (2H, m, CH_2), 2.92–3.03 (2H, m, CH_2).

Ring-opening reaction of *N*-acetylisatin 2a–d. Phenylalanyl phenylalanine methyl ester hydrochloride salt **9** was suspended in acetonitrile under a nitrogen atmosphere. Triethylamine was added as the base to neutralize the acid followed by addition of *N*-acetylisatin derivatives **2a–d**. The reaction mixture was stirred at room temperature for 10–15 minutes. Purification was conducted using column chromatography using hexane and ethyl acetate as the mobile phase to give **2a–d** as yellow solids.

Methyl (2-(2-acetamidophenyl)-2-oxoacetyl)-L-phenylalanyl-L-phenylalaninate **5a**: IR max 3295, 3260, 3060, 2948, 1740, 1688, 1632, 1582, 1528, 1450, 1366, 1259, 1208, 1160, 1118, 990, 913, 846, 743, 696 cm^{-1}; ^1H NMR (DMSO-d_6, 400 MHz) 10.68 (1H, s, NH), 8.95 (1H, d, *J* = 8.7 Hz, NH), 8.74 (1H, d, *J* = 7.8 Hz, NH), 8.14 (1H, d, *J* = 8.24 Hz, ArH), 7.62 (1H, td, *J* = 1.9, 8.7 Hz, ArH), 7.20–7.28 (10H, m, ArH), 7.00–7.09 (2H, m, ArH), 4.79 (1H, td, *J* = 10.0, 4.0 Hz, CH), 4.56 (1H, td, *J* = 8.4, 5.4 Hz, CH), 3.60 (3H, s, $COOCH_3$), 2.90–3.11 (2H, m, CH_2), 2.70–2.90 (2H, m, CH_2), 2.07 (3H, s, $COCH_3$). ^{13}C NMR (DMSO-d_6, 101 MHz) 192.47, 171.71, 170.51, 168.87, 163.95, 139.63, 137.27, 136.94, 134.84, 132.60, 129.32, 129.08, 128.32, 128.18, 126.65, 126.50, 122.85, 120.96, 120.62, 53.74, 53.30, 51.93, 37.65, 36.64, 24.43; HR-MS (ESI): calcd for $C_{29}H_{29}N_3O_6Na$: 538.1954, found 538.1942.

Methyl(2-(2-acetamido-5-fluorophenyl)-2-oxoacetyl)-L-phenylalanyl-L-phenylalaninate **5b**: IR max 3259, 3048, 2948, 1751, 1680, 1631, 1562, 1521,1445, 1356, 1257, 1206, 1160, 1110, 978, 912, 845, 742, 692 cm^{-1}; ^1H NMR (DMSO-d_6, 400 MHz) 10.44 (1H, s, *NH*), 8.79 (1H, d, *J* = 9.0 Hz, *NH*), 8.72 (1H, d, *J* = 7.8 Hz, *NH*), 7.87 (1H, dd, *J* = 9.1, 3.0 Hz, *ArH*), 7.48 (1H, td, *J* = 8.0, 3.3 Hz, *ArH*), 7.20–7.30 (10H, m, *ArH*), 7.03 (1H, dd, *J* = 9.1, 3.0 Hz, *ArH*), 4.70 (1H, td, *J* = 10.0, 4.0 Hz, *CH*), 4.56 (1H, td, *J* = 8.4, 5.4 Hz, *CH*), 3.61 (3H, s, $COOCH_3$), 2.99–3.11 (2H, m, CH_2), 2.83–2.99 (2H, m, CH_2), 2.00 (3H, s, $COCH_3$). ^{13}C NMR (DMSO-d_6, 101 MHz) 189.47, 171.66, 170.36, 168.71, 162.69, 137.20, 136.92, 134.85, 134.83, 129.28, 129.06, 128.30, 128.09, 126.63, 126.50, 124.66, 124.60, 123.74, 123.66, 121.13, 120.91, 117.43, 117.20, 53.71, 53.59, 51.90, 37.47, 36.65, 24.83; HR-MS (ESI): calcd for $C_{29}H_{28}FN_3O_6Na$: 533.1962, found 533.1950.

Methyl(2-(2-acetamido-5-methylphenyl)-2-oxoacetyl)-L-phenylalanyl-L-phenylalaninate **5c**: IR max 3265, 2922, 2464, 2113, 1920, 1729, 1635, 1591, 1526, 1444, 1305, 1222, 1208, 1175, 998, 913, 825, 751, 680 cm^{-1}; ^1H NMR (DMSO-d_6, 400 MHz) 10.57 (1H, s, *NH*), 8.93 (1H, d, *J* = 8.8 Hz, *NH*), 8.73 (1H, d, *J* = 7.7 Hz, *NH*), 8.00 (1H, d, *J* = 8.4 Hz, *ArH*), 7.41 (1H, dd, *J* = 8.4, 2.1 Hz, *ArH*), 7.20–7.32 (10H, m, *ArH*), 7.11 (1H, d, *J* = 2.1 Hz, *ArH*), 4.76 (1H, td, *J* = 10.0, 4.0 Hz, *CH*), 4.57 (1H, td, *J* = 8.4, 5.4 Hz, *CH*), 3.61 (3H, s, $COOCH_3$), 3.02–3.13 (2H, m, CH_2), 2.82–3.02 (2H, m, CH_2), 2.20 (3H, s, CH_3Ar), 2.03 (3H, s, $COCH_3$). ^{13}C NMR (DMSO-d_6, 101 MHz) 192.29, 171.68, 170.58, 168.66, 163.94, 137.33, 137.15, 136.95, 135.33, 132.35, 132.03, 129.25, 129.07, 128.30, 128.11, 126.64, 126.49, 121.41, 120.88, 53.75, 53.44, 51.89, 37.50, 36.66, 24.30, 20.16; HR-MS (ESI): calcd for $C_{30}H_{31}N_3O_6Na$: 552.2111, found 552.2105.

Methyl(2-(2-acetamido-5-bromophenyl)-2-oxoacetyl)-L-phenylalanyl-L-phenylalaninate **5d**: IR max 3227, 3038, 2933, 1741, 1656, 1624, 1512, 1511, 1432, 1327, 1287, 1211, 1143, 968, 915, 839, 721, 690 cm^{-1}; ^1H NMR (DMSO-d_6, 400 MHz) 10.51 (1H, s, *NH*), 8.75 (1H, d, *J* = 8.5 Hz, *NH*), 8.70 (1H, d, *J* = 7.6 Hz, *NH*), 7.75–7.81 (2H, m, *ArH*), 7.46 (1H, d, *J* = 2.13 Hz, *ArH*), 7.21–7.28 (10H, m, *ArH*), 4.67 (1H, td, *J* = 9.4, 3.7 Hz, *CH*), 4.56 (1H, td, *J* = 8.4, 5.4 Hz, *CH*), 3.61 (3H, s, $COOCH_3$), 3.01–3.07 (2H, m, CH_2), 2.84–3.01 (2H, m, CH_2), 2.00 (3H, s, $COCH_3$). ^{13}C NMR (DMSO-d_6, 101 MHz) 188.95, 171.63, 170.51, 170.28, 168.81, 162.36.63, 137.38, 137.15, 136.89, 136.45, 133.29, 129.22, 129.05, 128.29, 128.09, 126.62, 126.56, 125.16, 123.38, 114.71, 53.68, 53.63, 51.91, 37.41, 36.65, 23.91; HR-MS (ESI): calcd for $C_{29}H_{28}BrN_3O_6Na$: 616.1059, found 616.1042.

(2-(2-Acetamidophenyl)-2-oxoacetyl)-L-phenylalanyl-L-phenylalanine **6a**: IR max 3601, 3563, 3274, 3256, 3068, 3023, 2932, 1637, 1580, 1448, 1210, 1298, 1211, 1160, 983, 916, 839, 741, 677 cm^{-1}; ^1H NMR (DMSO-d_6, 400 MHz) 12.84 (1H, bs, COOH), 10.67 (1H, s, NH), 8.91 (1H, d, *J* = 8.7 Hz, NH), 8.57 (1H, d, *J* = 8.6 Hz, NH), 8.13 (1H, d, *J* = 8.6 Hz, ArH), 7.59 (1H, td, *J* = 8.6, 1.9 Hz, ArH), 7.20–7.28 (10H, m, ArH), 6.99–7.08 (2H, m, ArH), 4.78 (1H, td, *J* = 10.0, 4.0 Hz, CH), 4.51 (1H, td, *J* = 8.4, 5.4 Hz, CH), 2.97–3.14 (2H, m, CH_2), 2.76–2.92 (2H, m, CH_2), 2.06 (3H, s, $COCH_3$). ^{13}C NMR (DMSO-d_6, 101 MHz) 192.79, 171.72, 171.55, 170.56, 169.34, 164.21, 139.97, 138.05, 137.82, 135.15, 133.00, 129.82, 129.70, 128.60, 128.56, 126.87, 126.79, 123.34, 121.66, 121.11, 54.22, 53.92, 51.93, 41.17, 38.28, 24.84; HR-MS (ESI): calcd for $C_{29}H_{29}N_3O_6Na$: 524.1798, found 524.1785.

(2-(2-Acetamido-5-fluorophenyl)-2-oxoacetyl)-L-phenylalanyl-L-phenylalanine **6b**: IR max 3598, 3560, 3172, 3243, 3118, 3027, 2946, 2832, 1625, 1567, 1432, 1209, 1298, 1203, 1154, 974, 910, 825, 740, 677 cm^{-1}; ^1H NMR (DMSO-d_6, 400 MHz) 12.81 (1H, bs, *COOH*), 10.43 (1H, s, *NH*), 8.76 (1H, d, *J* = 8.8 Hz, *NH*), 8.58 (1H, d, *J* = 7.8 Hz, *NH*), 7.87 (1H, dd, *J* = 9.1, 5 Hz, *ArH*), 7.48 (1H, td, *J* = 8.0, 3.3 Hz, *ArH*), 7.21–7.29 (10H, m, *ArH*), 7.02 (1H, dd, *J* = 9.1, 3.0 Hz *ArH*), 4.70 (1H, td, *J* = 10.0, 4.0 Hz, *CH*), 4.52 (1H, td, *J* = 8.4, 5.4 Hz, *CH*), 3.07–3.15 (2H, m, CH_2), 2.83–2.99 (2H, m, CH_2), 2.00 (3H, s, $COCH_3$). ^{13}C NMR (DMSO-d_6, 101 MHz) 189.47, 172.72, 172.65, 171.46, 170.22, 168.70, 162.63, 155.89, 137.41, 137.32, 137.24, 134.83, 129.32, 129.11, 128.23, 128.18, 128.06, 127.96, 126.50, 126.16, 124.73, 124.66, 123.74, 123.66 121.10, 120.88, 117.42, 117.18, 54.22, 53.61, 53.58, 37.52, 36.71, 23.81, 22.40; HR-MS (ESI): calcd for $C_{28}H_{26}FN_3O_6$ Na: 542.1703, found 542.1712.

(2-(2-Acetamido-5-methylphenyl)-2-oxoacetyl)-L-phenylalanyl-L-phenylalanine **6c**: IR max 3260, 3023, 2768, 2416, 2112, 1728, 1633, 1590, 1525, 1443, 1405, 1368, 1317, 1221, 1174, 1015, 837, 825, 776, 716, 698 cm^{-1}; ^1H NMR (DMSO-d_6, 400 MHz) 10.54 (1H, s, *NH*), 8.88 (1H, d, *J* = 8.6 Hz, *NH*), 8.54 (1H, d, *J* = 8.6 Hz, *NH*), 7.97 (1H, d, *J* = 8.5 Hz, *ArH*), 7.41 (1H, dd, *J* = 8.5, 1.8 Hz, *ArH*), 7.19–7.30 (10H, m, *ArH*), 7.07 (1H, d, *J* = 2 Hz *ArH*), 4.74 (1H, td, *J* = 10.0, 4.0 Hz, *CH*), 4.50 (1H, td, *J* = 8.4, 5.4 Hz, *CH*), 3.05–3.13 (2H, m, CH_2), 2.80–3.05 (2H, m, CH_2), 2.18 (3H, s, CH_3Ar), 2.03 (3H, s, $COCH_3$). ^{13}C NMR (DMSO-d_6, 101 MHz) 192.74, 173.12, 170.91, 170.56, 169.12, 164.36, 137.86, 137.81, 137.82, 137.58, 135.56, 132.79, 132.50, 129.75, 129.60, 128.70, 128.55, 126.97, 126.93, 121.93, 121.36, 54.07, 53.93, 37.98, 37.16, 24.75, 20.64; HR-MS (ESI): calcd for $C_{29}H_{29}N_3O_6Na$: 538.1954, found 538.1942.

(2-(2-Acetamido-5-bromophenyl)-2-oxoacetyl)-L-phenylalanyl-L-phenylalanine **6d**: IR max 3152, 3021, 2698, 2411, 2126, 1720, 1642, 1578, 1511, 1442, 1413, 1376, 1315, 1223, 1175, 833, 819, 765, 716, 690 cm^{-1}; ^1H NMR (DMSO-d_6, 400 MHz) 10.51 (1H, s, *NH*), 8.72 (1H, d, J = 8.6 Hz, *NH*), 8.67 (1H, d, J = 7.6 Hz, *NH*), 7.77–7.78 (2H, m, *ArH*), 7.44 (1H, d, J = 2.2 Hz, *ArH*), 7.18–7.29 (10H, m, *ArH*), 4.69 (1H, td, J = 10.0, 4.0 Hz, *CH*), 4.51 (1H, td, J = 8.4, 5.4 Hz, *CH*), 3.05–3.14 (2H, m, CH_2), 2.84–2.98 (2H, m, CH_2), 1.99 (3H, s, $COCH_3$). ^{13}C NMR (DMSO-d_6, 101 MHz) 189.45, 173.10, 170.65, 170.56, 169.30, 162.80, 137.86, 137.77, 137.68, 136.91, 133.75, 129.76, 129.59, 128.71, 128.54, 126.98, 125.68, 123.87, 115.21, 54.12, 54.04, 53.93, 37.94, 37.19, 24.38; HR-MS (ESI): calcd for $C_{28}H_{26}BrN_3O_6Na$: 602.0903, found 602.0911.

Preparation of organogel

To a vial containing a pre-weighed compound, 1 mL solvent was added. The vial was heated for approximately 5–10 minutes using a heat gun, resulting in dissolution of the compound. The vial was then left at room temperature for 5–30 min for the gelation process to occur. The vial was inverted and allowed to stand overnight to confirm the gelation process.

Preparation of hydrogel

To the pre-weighed compound, 0.1 M NaOH (1.5 eq.) was added. The solution was vortexed for 5 min to dissolve the compound. This solution was then transferred to a vial containing 3 eq. of GdL. The resulting solution was allowed to stand for 30 min. The vial was inverted and allowed to stand overnight to confirm the gelation process.

FTIR measurement

ATR-FTIR spectra were collected using a Spectrum 100 FTIR spectrometer (PerkinElmer, USA) fitted with a 1 mm diamond-ZnSe crystal. The spectrum of the xerogel of **5a** was recorded from 4000–650 cm^{-1} with 4 cm^{-1} resolutions and 1 scan. The spectrum of the toluene gel of **5a** (in 0.1 wt%) was recorded by applying a pre-formed gel to the ATR crystal and protecting from evaporation by covering with a KBr disk, then measured from 4000–650 cm^{-1} with 4 cm^{-1} resolutions and 32 scans. The final spectrum was obtained by subtracting a spectrum of pure toluene.

In situ FTIR measurement

Fourier transform infrared (FTIR) spectroscopy was performed on a Spectrum 100 FTIR (PerkinElmer, UK) fitted with a diamond-ZnSe attenuated total reflectance crystal at ambient temperature using 16 accumulations from 4000 to 650 cm^{-1} with a spectral resolution of 4 cm^{-1}. The gel was warmed to 50 °C until fluid, then a single drop placed on the crystal where it immediately cooled. Spectra were collected over a 22 minute period and processed using Spectrum 10 software (PerkinElmer, UK).

CD measurement

Both organogels and hydrogels were prepared at 0.5% w/v, and were diluted by 8× in the respective solvent (2-propanol or water, respectively) before being transferred into a 0.1 mm length cuvette. The data was collected using a ChirascanPlus CD spectrometer (Applied Photophysics, UK) scanning between wavelengths of 180–500 nm with a bandwidth of 1 nm, 0.6 s per point, and step of 1 nm. Each experiment was repeated three times and the results were averaged into a single plot value.

UV/Vis measurement

The subtle red shift of the peptide mimic solution was measured using an Agilent Cary 60 UV-Vis spectrometer with concentrations ranging from 0.01 mg mL^{-1} to 0.5 mg mL^{-1}.

Rheology measurement

Mechanical properties and T_g values of all the gels obtained were examined using an Anton Paar MCR 302 rheometer with 25 mm stainless steel parallel plate configuration. 550 μL of 0.5% w/v gel (in the solution phase) was cast onto the plate. The other plate was lowered to the measuring position (1 mm) and the solution was allowed to stand for 5 min for the gel to be formed. To prevent the evaporation of the solvent, a solvent trap using MilliQ water was employed, as was a Peltier temperature controlled hood. The frequency sweep test was conducted using 10 Hz to 0.01 Hz frequency at a constant strain of 0.2%. Besides, strain sweep tests were performed using 0.1% to 100% strain with a constant frequency of 1 Hz. Additionally, the temperature sweep test, to determine the T_g, was conducted using temperature ramping from 10–65 °C with a constant frequency of 1 Hz and a constant strain of 0.2% strain. The rheology data shown are an average of three repeats for each point.

AFM measurement

Organogels were prepared beforehand then heat was re-applied to transform the gels back into their solution phase. One drop of the organo-gel in its solution phase was cast onto a mica substrate. A glass slide was used to spread the droplets and left to dry overnight before imaging. The hydrogels were prepared in a similar manner, except that the hydrogels were cast right after the addition of GdL and before the gelation occurred. Imaging was undertaken on a Bruker Mulitmode 8 Atomic Force Microscope in Scanasyst Air (PeakForce Tapping®) mode, which is based upon tapping mode AFM, but whereby the imaging parameters are constantly optimised through the force curves that are collected, preventing damage of soft samples. Bruker Scanasyst-Air probes were used, with a spring constant of 0.4–0.8 N m^{-1} and a tip radius of 2 nm.

Powder X-ray diffraction

Powder X-ray diffraction measurements were undertaken on a PANalytical Xpert Multipurpose X-ray diffraction system, using Mo Kα radiation and scanning from 5 to 50 degrees. Samples were prepared in a steel sample holder and either dried over 48 h for xerogels or left to gel for 2 h to obtain native gel samples before measurements.

Cell biology techniques

The human lung fibroblast cell line MRC-5 was cultured in MEM medium (invitrogen) supplemented with 10% FCS, 1% L-glutamine, 2% sodium bicarbonate, 1% medium NEAA and 1% sodium pyruvate. All cell lines were maintained at 37 °C in 5% CO_2 as an adherent monolayer and were passaged upon reaching confluence by using standard cell culture techniques.

Cell viability assays

MRC-5 cells were seeded at 20 000 cells per well in 96-well plates to ensure full confluence (quiescence) for the cytotoxicity assay. Cells were treated 24 h after seeding with a concentration between 0.01 and 1.0% w/v of the compounds. After 72 h drug assay the cells were treated 24 h after seeding with a concentration between 0.01 and 1.0% w/v of the compounds. After 72 h drug incubation, the treatment medium was replaced with 10% Alamar blue in fresh medium and the cells were incubated for another 6 h. The metabolic activity was detected by spectrophotometric analysis by assessing the absorbance of Alamar blue as previously described.[29] Cell proliferation and viability was expressed as a percentage of untreated control cells. The determination of IC_{50} values was performed using GraphPad Prism 6 (San Diego, CA, USA).

Statistical analysis

All *in vitro* experiments were performed at least in triplicate and statistical significance was determined using the two-sided Student's *t* test. All statistical analyses were performed using GraphPad Prism 6 (GraphPad Software, Inc.).

Conflicts of interest

There are no conflicts of interest to declare.

Acknowledgements

The authors would like to acknowledge the Indonesia Endowment Fund for Education (LPDP) for the PhD Scholarship given to VRA and the Mark Wainwright Analytical Centre facilities at UNSW Australia for supporting the characterisation of the synthesised compounds.

References

1 W. T. Truong, Y. Su, J. T. Meijer, P. Thordarson and F. Braet, *Chem. – Asian J.*, 2011, **6**, 30–42.
2 L. Adler-Abramovich and E. Gazit, *Chem. Soc. Rev.*, 2014, **43**, 6881–6893.
3 C. Tomasini and N. Castellucci, *Chem. Soc. Rev.*, 2013, **42**, 156–172.
4 S. Fleming and R. V. Ulijn, *Chem. Soc. Rev.*, 2014, **43**, 8150–8177.
5 V. Jayawarna, M. Ali, T. A. Jowitt, A. F. Miller, A. Saiani, J. E. Gough and R. V. Ulijn, *Adv. Mater.*, 2006, **18**, 611–614.
6 M. C. Branco and J. P. Schneider, *Acta Biomater.*, 2009, **5**, 817–831.
7 S. Marchesan, A. V. Vargiu and K. E. Styan, *Molecules*, 2015, **20**, 19775–19788.
8 K. J. Skilling, F. Citossi, T. D. Bradshaw, M. Ashford, B. Kellam and M. Marlow, *Soft Matter*, 2014, **10**, 237–256.
9 B. Adhikari and A. Banerjee, *Chem. – Eur. J.*, 2010, **16**, 13698–13705.
10 H. Vilaça, A. C. Hortelão, E. M. Castanheira, M. R. Queiroz, L. Hilliou, I. W. Hamley, J. A. Martins and P. M. Ferreira, *Biomacromolecules*, 2015, **16**, 3562–3573.
11 Z. Yang, G. Liang and B. Xu, *Acc. Chem. Res.*, 2008, **41**, 315–326.
12 E. R. Draper, T. O. McDonald and D. J. Adams, *Chem. Commun.*, 2015, **51**, 6595–6597.
13 S. M. Hsu, Y. C. Lin, J. W. Chang, Y. H. Liu and H. C. Lin, *Angew. Chem., Int. Ed.*, 2014, **53**, 1921–1927.
14 E. K. Johnson, D. J. Adams and P. J. Cameron, *J. Mater. Chem.*, 2011, **21**, 2024–2027.
15 M. Reches and E. Gazit, *Isr. J. Chem.*, 2005, **45**, 363–371.
16 S. Fleming, S. Debnath, P. W. Frederix, T. Tuttle and R. V. Ulijn, *Chem. Commun.*, 2013, **49**, 10587–10589.
17 C. Tang, A. M. Smith, R. F. Collins, R. V. Ulijn and A. Saiani, *Langmuir*, 2009, **25**, 9447–9453.
18 A. D. Martin, J. P. Wojciechowski, H. Warren and P. Thordarson, *Soft Matter*, 2016, **12**, 2700–2707.
19 S.-M. Hsu, J.-W. Chang, F.-Y. Wu, Y.-C. Lin, T.-S. Lai, H. Cheng and H.-C. Lin, *RSC Adv.*, 2015, **5**, 32431–32434.
20 A. D. Martin, A. B. Robinson and P. Thordarson, *J. Mater. Chem. B*, 2015, **3**, 2277–2280.
21 W. C. Cheah, D. S. Black, W. K. Goh and N. Kumar, *Tetrahedron Lett.*, 2008, **49**, 2965–2968.
22 A. D. Martin, A. B. Robinson, A. F. Mason, J. P. Wojciechowski and P. Thordarson, *Chem. Commun.*, 2014, **50**, 15541–15544.
23 F. Sun, G. Zhang and D. Zhang, *Chin. Sci. Bull.*, 2012, **57**, 4284–4288.
24 S. V. Jadhav, P. Amabili, H.-G. Stammler and N. Sewald, *Chem. – Eur. J.*, 2017, **23**, 10352–10357.
25 L. M. De Leon-Rodriguez, Y. Hemar, G. Mo, A. K. Mitra, J. Cornish and M. A. Brimble, *Acta Biomater.*, 2017, **47**, 40–49.
26 W. Suida, *Ber. Dtsch. Chem. Ges.*, 1878, **11**, 584–587.
27 W. C. Cheah, K. Wood, D. S. Black and N. Kumar, *Tetrahedron*, 2011, **67**, 7603–7610.
28 Y. Wang, Z. Zhang, L. Xu, X. Li and H. Chen, *Colloids Surf., B*, 2013, **104**, 163–168.
29 D. J. Adams, M. F. Butler, W. J. Frith, M. Kirkland, L. Mullen and P. Sanderson, *Soft Matter*, 2009, **5**, 1856–1862.
30 G. Fichman and E. Gazit, *Acta Biomater.*, 2014, **10**, 1671–1682.
31 D. J. Adams, L. M. Mullen, M. Berta, L. Chen and W. J. Frith, *Soft Matter*, 2010, **6**, 1971–1980.
32 N. Singh, M. Kumar, J. F. Miravet, R. V. Ulijn and B. Escuder, *Chem. – Eur. J.*, 2016, **23**, 981–993.
33 S. Maity, P. Das and M. Reches, *Sci. Rep.*, 2015, **5**, 16365.
34 D. M. Ryan, T. M. Doran, S. B. Anderson and B. L. Nilsson, *Langmuir*, 2011, **27**, 4029–4039.
35 B. A. Chromy, R. J. Nowak, M. P. Lambert, K. L. Viola, L. Chang, P. T. Velasco, B. W. Jones, S. J. Fernandez, P. N. Lacor and P. Horowitz, *Biochemistry*, 2003, **42**, 12749–12760.

36 M. Krysmann, V. Castelletto, J. McKendrick, L. Clifton, P. Harris and S. King, *Langmuir*, 2008, **24**, 8158–8162.
37 M. Gupta, A. Bagaria, A. Mishra, P. Mathur, A. Basu, S. Ramakumar and V. S. Chauhan, *Adv. Mater.*, 2007, **19**, 858–861.
38 S.-Y. Qin, Y. Pei, X.-J. Liu, R.-X. Zhuo and X.-Z. Zhang, *J. Mater. Chem. B*, 2013, **1**, 668–675.
39 S.-Y. Qin, Y.-F. Chu, L. Tao, S.-S. Xu, Z.-Y. Li, R.-X. Zhuo and X.-Z. Zhang, *Soft Matter*, 2011, **7**, 8635–8641.
40 J. Keen and T. B. McLeish, *J. Mater. Chem.*, 1997, **7**, 1135–1145.
41 S. Brahms and J. Brahms, *J. Mol. Biol.*, 1980, **138**, 149–178.
42 M. Diem, *Modern vibrational spectroscopy and micro-spectroscopy: theory, instrumentation and biomedical applications*, John Wiley & Sons, 2015.
43 G. Fichman and E. Gazit, *Acta Biomater.*, 2014, **10**, 1671–1682.
44 D. M. Ryan, S. B. Anderson and B. L. Nilsson, *Soft Matter*, 2010, **6**, 3220–3231.
45 M. J. Thompson, J. C. Louth, S. Ferrara, M. P. Jackson, F. J. Sorrell, E. J. Cochrane, J. Gever, S. Baxendale, B. M. Silber and H. H. Roehl, *Eur. J. Med. Chem.*, 2011, **46**, 4125–4132.
46 S. Nizalapur, K. K. Ho, Ö. Kimyon, E. Yee, T. Berry, M. Manefield, C. G. Cranfield, M. Willcox, D. S. Black and N. Kumar, *Org. Biomol. Chem.*, 2016, **14**, 3623–3637.
47 T. Zohrabi, N. Habibi, A. Zarrabi, M. Fanaei and L. Y. Lee, *J. Biomed. Mater. Res., Part A*, 2016, **104**, 2280–2290.
48 Y. Liu, Y. Zhang, Z. Wang, J. Wang, K. Wei, G. Chen and M. Jiang, *J. Am. Chem. Soc.*, 2016, **138**, 12387–12394.